Adjuvant Therapy with Small Hairpin RNA Interference Prevents Non–Small Cell Lung Cancer Metastasis Development in Mice

Etmar Bulk,[1] Antje Hascher,[1] Ruediger Liersch,[1] Rolf M. Mesters,[1] Sven Diederichs,[4] Bülent Sargin,[1] Volker Gerke,[3] Marc Hotfilder,[2] Josef Vormoor,[5] Wolfgang E. Berdel,[1] Hubert Serve,[1] and Carsten Müller-Tidow[1]

Departments of [1]Medicine, Hematology and Oncology, [2]Pediatric Hematology and Oncology, and [3]Medical Biochemistry, University of Münster, Münster, Germany; [4]Massachusetts General Hospital Cancer Center, Harvard Medical School, Charlestown, Massachusetts; and [5]Northern Institute for Cancer Research, Newcastle University, Newcastle upon Tyne, United Kingdom

Abstract

Development of distant metastasis is the major reason for cancer-related deaths worldwide. Adjuvant therapy approaches after local therapies are most effective when specific targets are inhibited. Recently, we identified S100P overexpression as a strong predictor for metastasis development in early-stage non–small cell lung cancer (NSCLC) patients. Here, we show that S100P overexpression increased angiogenesis in and metastasis formation from s.c. xenotransplants of NSCLC cells. Plasmid-derived short hairpin RNAs (shRNA) were developed as specific adjuvant therapy. I.v. injected shRNA against S100P significantly decreased S100P protein expression in xenograft tumors and inhibited tumor angiogenesis *in vivo*. Metastasis formation 8 weeks after primary tumor resection was significantly reduced. Lung metastases developed in 31% of mice treated with S100P-targeting shRNAs compared with 64% in control shRNA–treated mice ($P < 0.05$). These findings suggest that RNA interference–based therapy approaches can be highly effective in the adjuvant setting. [Cancer Res 2008;68(6):1896–904]

Introduction

Distant metastases are a major reason for cancer-related death in patients with solid tumors (1). Adjuvant therapy applied after local tumor therapy can prolong survival in a substantial fraction of patients with solid tumors. However, specific therapeutic approaches are currently available only for a minority of patients. Non–small cell lung cancer (NSCLC) ranks among the most common cancers and is associated with a complex pathogenesis (2). In patients with stage I and II NSCLC, ~50% of patients are cured by surgery alone (3). The frequent use of computed tomography (CT) scanning and a renewed interest in screening by low-dose CT scanning have led to an increase in the number of patients that present with early-stage NSCLC that is potentially curable (4). Despite the absence of lymph node involvement and small tumor size, a considerable fraction of patients eventually develop metastasis. Adjuvant chemotherapy can be administered to improve outcome in this patient population. Recently, several large clinical trials showed a small but significant improvement in survival of NSCLC patients with stage Ib and II tumors treated with adjuvant chemotherapy (5, 6). However, it is clear that adjuvant chemotherapy benefits only a minor group of patients. It lacks benefit for the patients that eventually metastasize anyway and it might have adverse effects in patients that would not have developed metastasis even without adjuvant chemotherapy. Improvement of adjuvant chemotherapy can derive from a better identification of patients at risk and from more specific approaches that specifically target the metastatic process. An excellent example is the high effectivity of adjuvant trastuzumab therapy in Her2/Neu-positive breast cancer (7). To develop improved adjuvant therapy options for NSCLC, relevant targets need to be identified and gene-specific therapies need to be developed.

As a step toward this goal, we recently identified genes whose expression in primary NSCLC was associated with a high risk of metastasis development (8, 9). High levels of S100P expression were closely correlated with metastasis development and NSCLC-related death. The association between S100P expression and a more aggressive tumor phenotype was also reported for several other tumor entities (10–13). In the current study, we show that S100P induces a metastatic phenotype in NSCLC cells *in vivo*. Metastasis induction is associated with increased angiogenesis found in S100P-expressing tumors. In a mouse model for adjuvant NSCLC treatment, small hairpin RNA interference (RNAi) against S100P inhibited angiogenesis, reduced tumor growth, and inhibited metastasis formation by >50%. These findings show that S100P is an important metastasis mediator in NSCLC and that short hairpin RNAi can be used as adjuvant therapy to specifically target metastasis development.

Materials and Methods

Cell culture. HTB56 and HTB58 lung adenocarcinoma cells were cultured at 37°C, high humidity, and 5% CO_2 in MEM (Invitrogen). The medium was supplemented with 10% FCS, 1% streptomycin and penicillin, 1% glutamine, 1% sodium pyruvate, and 1% nonessential amino acid. HMEC-1 cells were cultured at 37°C, high humidity, and 3% CO_2 using MCDB 131 medium (Invitrogen) with 1% streptomycin and penicillin, 5% glutamine, 10% FCS Gold, and 50 μg/mL gentamicin. BXPC-3 cells were cultured at 37°C, high humidity, and 5% CO_2 in RPMI 1640 (Biochrom AG) containing 10% FCS, 1% glutamine, and 1% streptomycin and penicillin.

Cloning and transfection. Coding sequences of S100P (NM_005980), SEC61β (NM_006808), and EIF4A1 (NM_001416) were cloned into the expression vector pcDNA3.1(+), fused with the enhanced green fluorescent protein (EGFP). The cloned constructs were stably transfected into HTB56 (Calu6) with Lipofectamine reagent (Invitrogen) and selected with neomycin (G418; Sigma). To avoid clone-specific effects, bulk cultures were used for all experiments. Expression levels were determined by quantitative real-time reverse transcription-PCR (RT-PCR) and Western blotting.

Requests for reprints: Carsten Müller-Tidow, Department of Medicine A, Hematology and Oncology, University of Münster, Domagkstr. 3, 48129 Münster, Germany. Phone: 49-251-835-2995; Fax: 49-251-835-2673; E-mail: muellerc@uni-muenster.de.

doi:10.1158/0008-5472.CAN-07-2390

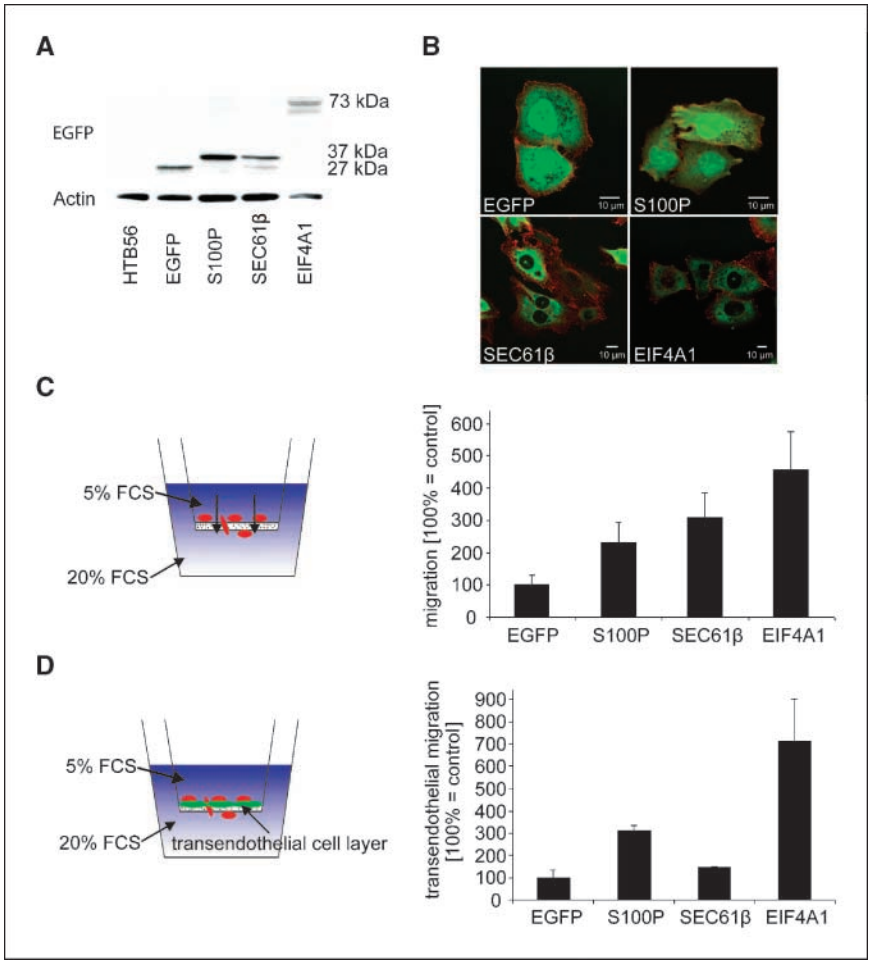

Figure 1. Generation of stable cell lines in HTB56. *A,* protein expression by Western blotting of the stably transfected HTB56 NSCLC cell lines expressing EGFP, EGFP-S100P, EGFP-SEC61β, or EGFP-EIF4A1. *B,* confocal microscopy of the HTB56 cells after counterstaining with TRITC-phalloidin. Red staining with TRITC-phalloidin visualizes the actin cytoskeleton. *Green,* protein localization is visualized by fluorescence of the EGFP fusion protein. *C,* Transwell migration of the different cell lines toward a high serum gradient. *Right,* percentages of migrated cells. Cells stably transfected into pcDNA3.1(+), fused with EGFP, were used as control cells. *Columns,* mean of three independent experiments performed in triplicate ($P = 0.026$, ANOVA); *bars,* SD. *D,* transendothelial migration through an endothelial cell layer. *Left,* principle of the transendothelial migration. Transwell filters were precoated with HMEC-1 cells forming a confluent transendothelial cell layer. The different NSCLC lines were loaded with the red fluorescent dye SNARF and added into the upper part of the Transwell chamber. Only SNARF-positive cells were analyzed using flow cytometry after 16 h of migration. The diagram shows the results of three independent experiments made in triplicate. Cells stably transfected into pcDNA3.1(+), fused with EGFP, were used as control cells. *Columns,* mean of three independent experiments performed in triplicate; *bars,* SD.

Silencing of gene expression was achieved using short hairpin RNA (shRNA) technology. Oligonucleotides targeting S100P_1 (sense, TGCCGTGGATAAATTGCTCAA; antisense, TTGAGCAATTTATCCACGGCA; loop, TTGATATCCG), S100P_2 (sense, AATGGAGATGCCCAGGTGGAC; antisense, GTCCACCTGGGCATCTCCATT; loop, AAGCTT), and the scrambled control (sense, AGATCCGTATAGTGTACCTTA; antisense, TAAGGTACACTATACGGATCT; loop, TTGATATCCG) were synthesized by Invitrogen, annealed, and cloned into the shRNA expression vector pRNAT-H1.1/Neo (GenScript). HTB58 cells were transfected and selected as described above. Expression levels were verified by quantitative real-time RT-PCR. For Western blot analysis, BXPC-3 cells that express S100P at a high level were transfected as described (14).

Immunofluorescence staining. Stably transfected human HTB56 lung carcinoma cells were grown overnight on coverslips in MEM. Cells were fixed in 4% paraformaldehyde, permeabilized in 0.2% Triton X-100, stained for 15 min with tetramethylrhodamine isothiocyanate (TRITC)-phalloidin, and embedded in Mowiol 4-88 (Calbiochem). The stained slides were analyzed using the laser scanning confocal microscope Zeiss LSM-510.

Gene expression analysis. Analysis of gene expression was performed using quantitative RT-PCR as described (15). The following primer and probes (FAM and TAMRA labeled) were used for S100P: forward, 5′-GCTGATGGAGAAGGAGCTACCA; reverse, 5′-CCAGGTCCTTGAGCAATTTATCC; and probe, 5′-FAM-TCCTGCAGAGTGGAAAAGACAAGGATGC-TAMRA. The mRNA expression levels were calculated with regard to the internal standard of glyceraldehyde-3-phosphate dehydrogenase as described (16). Primer and, where applicable, probe sequences for the other S100 proteins will be provided on request.

Western blot analysis. Proteins were detected using the following antibodies: S100P,[6] GFP (Santa Cruz Biotechnology), signal transducer and activator of transcription 5 (Stat5; Santa Cruz Biotechnology), and actin (Sigma-Aldrich) as first antibodies and goat anti-mouse and goat anti-rabbit (both from Dianova) as secondary antibodies. Western blot analysis was carried out as described (15).

Migration assay. A total of 5×10^5 cells (in 100 μL MEM with 5% FCS) were seeded into the upper part of a Transwell chamber (Transwell filter inserts in 6.5-mm diameter with a pore size of 5 μm; Corning, Inc.), which was 30 min precoated with 50 μg fibronectin. In the lower part of the chamber, 600 μL MEM with 20% FCS was added and the assay was performed for 16 h at 37°C and 5% CO_2 before migrated cells were analyzed by flow cytometry. For the migration assay using transendothelial cells, Transwell filters were precoated with 2.2×10^5 HMEC-1 cells for 48 h at 37°C and 3% CO_2, forming a confluent transendothelial cell layer (17). NSCLC cells (5×10^5) were stained for 5 min with 5 μmol/L SNARF (1 carboxylic acid, acetate, succinimidyl ester; Molecular Probes) to avoid counting fragments of endothelial cells and added to the upper part of the Transwell chamber coated with transendothelial cells. After 16 h of migration, cells were harvested by trypsinization and analyzed (only SNARF-positive cells) by flow cytometry. All assays were performed in triplicate and independently performed thrice.

Metastasis experiments *in vivo*. For all mouse experiments, we used 8- to 10-wk-old NOD.CB17-Prkdc<scid>/J [nonobese diabetic/severe

[6] V. Gerke et al., unpublished data.

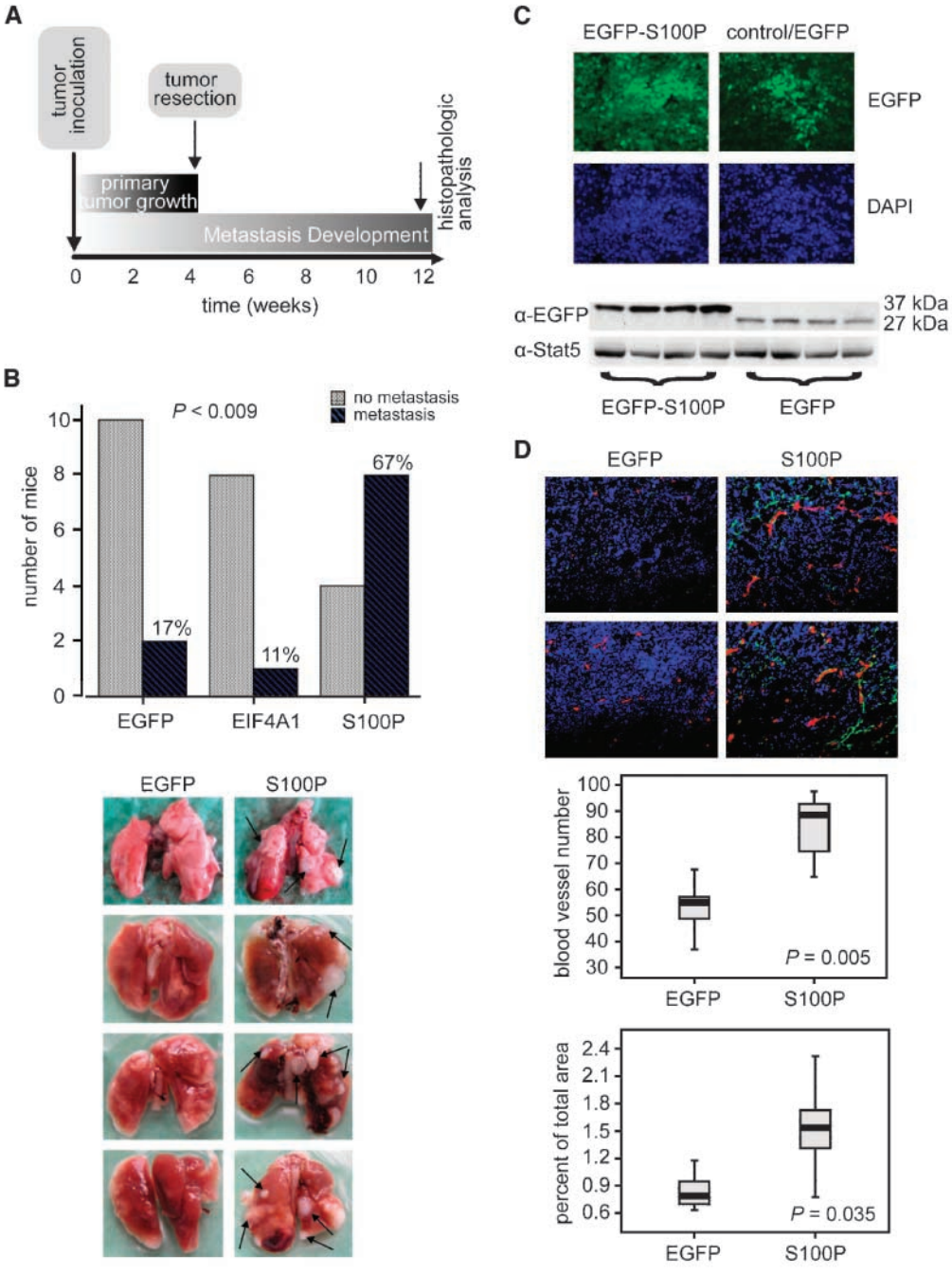

Figure 2. Tumor growth and metastasis development in mice. *A,* metastasis model of NOD/SCID mice. Four weeks after s.c. tumor inoculation, the tumor was surgically removed. Metastasis formation was analyzed 8 wk after surgery by histopathologic analyses. *B,* metastasis formation after surgery in NOD/SCID mice. Twelve weeks after tumor inoculation and 8 wk after tumor resection, the mice were sacrificed and analyzed. Mice inoculated with S100P-expressing tumors ($n = 12$) developed significantly more metastasis than mice inoculated with EGFP-expressing control cells ($n = 12$) or EIF4A1-overexpressing cells ($n = 9$). *Top, black columns,* mice that harbored lung metastasis ($P < 0.009$, Fischer's exact test; three groups). *Bottom,* photographs of lungs 12 wk after tumor inoculation. *Black arrows,* metastases. *C,* EGFP expression in excised tumor samples from NOD/SCID mice. Frozen sections from excised tumors (*top*) show EGFP expression indicating continuous expression of the transgene. Counterstaining was performed with 4′,6-diamidino-2-phenylindole (*DAPI*). *Bottom,* protein expression of S100P and EGFP in tumor samples of NOD/SCID mice. Tumor samples were crushed and lysed in radioimmunoprecipitation assay buffer. Antibodies against EGFP (Santa Cruz Biotechnology) and total Stat5 (Santa Cruz Biotechnology) as a loading control were used. The sizes of the S100P-EGFP fusion protein and EGFP alone are indicated. *D,* angiogenesis in tumor samples of NOD/SCID mice. *Top,* frozen sections were stained with SMA-1 (Alexa green) and CD31 (Alexa red). *Blue,* DAPI was used for nuclear staining. EGFP fluorescence was lost due to fixation. *EGFP,* control vector tumors harboring the control vector that were compared with S100P-containing tumors. Magnification, ×200. Two representative examples of each tumor type are shown. *Red,* blood vessel formation was induced by S100P, recognizable by specific marker as CD31. Green marked areas give morphologic localization of newly generated smooth muscle cells (SMA). *Middle,* S100P has proangiogenic properties. The figure shows the number of blood vessels in tumor samples of NOD/SCID mice. Computer-based fluorescence analyses indicate the total number of blood vessels. Out of five different tumor samples, mean values were calculated by the Image-Pro Plus software (Media Cybernetics). Blood vessel numbers of EGFP (control) and S100P-expressing tumors are shown in the box plot diagrams ($P = 0.005$, t test). *Bottom,* the areas covered by blood vessels were analyzed and are indicated as the percentage of the total area ($P = 0.035$, t test).

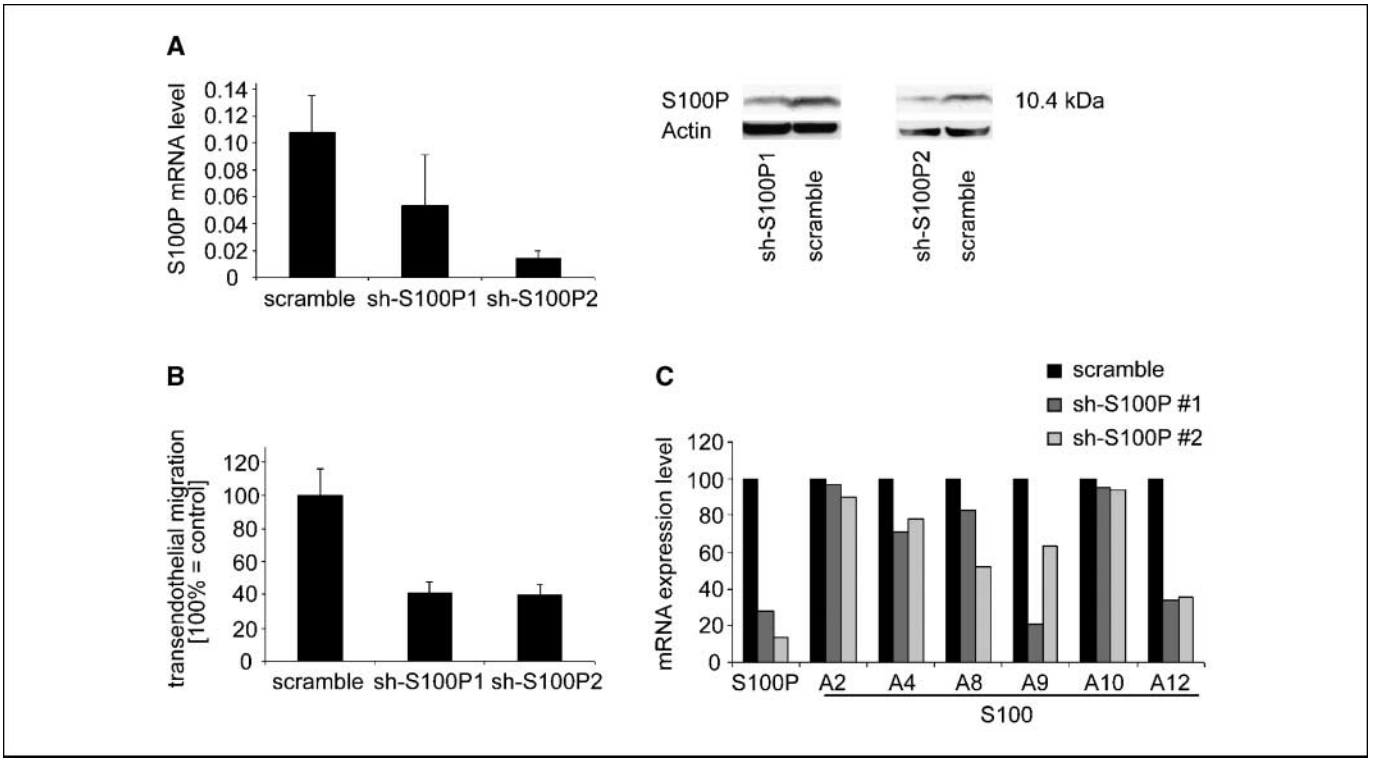

Figure 3. Effectivity of shRNA against S100P *in vitro. A,* down-regulation of S100P by shRNA in HTB58 cells. *Left,* mRNA levels for S100P were analyzed by quantitative RT-PCR; *right,* Western blot analysis of BXPC-3 cells transfected with shRNAs for S100P or the scrambled control shRNA. Endogenous S100P expression was >30-fold higher in this pancreatic cell line compared with NSCLC cells. The significant decrease of S100P by the specific shRNAs was confirmed by densitometry [shRNA-S100P1 (*sh-S100P1*), 0.03; scramble, 0.086; shRNA-S100P2 (*sh-S100P2*), 0.076; scramble, 0.236 absorbance]. *B,* shRNA for S100P decreases transendothelial migration in HTB58 cells. Cells were stained with SNARF before adding to the upper chamber (precoated with transendothelial cells). Only SNARF-positive cells were analyzed by flow cytometry. *Columns,* mean of two independent experiments performed in triplicate ($P = 0.029$); *bars,* SD. Cells stably transfected with the scrambled shRNA were used as control. *C,* specificity of S100P-shRNAs against other S100 proteins. Using RT-PCR, several genes of S100 proteins were tested in cDNAs from HTB58 and BXPC-3 cells transfected with shRNAs for S100P. *Columns,* means of the mRNA expression levels in both cell lines with scrambled shRNA for each gene set as 100.

combined immunodeficient (NOD/SCID)] mice obtained either by breeding in our in-house facility or from Charles River.

To analyze metastasis development following primary tumor removal, 2.5×10^6 stably transfected NSCLC cells (supplemented in 200 μL PBS) were injected s.c. into the right flank. After 4 wk of tumor growth, primary tumors were surgically removed and the tumor weight (g) was determined. Mice were followed for an additional 8 wk (12 wk after initial tumor injection). At this time, mice were sacrificed and tumor weight and metastasis development were determined. Metastasis development was evaluated by counting individual metastatic nodules. For histologic analyses, the lungs were frozen or fixed in 4% paraformaldehyde and embedded in paraffin. For adjuvant therapy experiments, mice were treated by i.v. injection of 20 μg shRNA (dissolved in 200 μL of 0.9% NaCl solution) twice in the week before surgery, during surgery (after primary tumor removal), and twice in the week after surgery. To analyze shRNA effects on metastasis development on i.v. tumor cell injection, NOD/SCID mice were irradiated with a single dose of 3.5 Gy from a cobalt-60 unit 1 d before transplantation. A total of 2×10^6 stable transfected cells (EGFP, control cells, dissolved in 200 μL PBS) were injected i.v. into the tail vein. One week after transplantation, 20 μg shRNA (dissolved in 250 μL PBS) was i.v. injected. Treatment with shRNA was repeated four times every fourth day. After the treatment, mice were followed for an additional 5 wk before metastasis development was analyzed. In a few cases, mice died during i.v. injection or surgery. Therefore, the number of the mice differs by one or two. None of the mice died in the weeks after shRNA injection. In all experiments, treatment groups were randomized to prevent cage effects.

Angiogenesis analysis. Angiogenesis was analyzed by immunofluorescence staining of frozen sections of the primary tumors. In brief, cryosections were fixed in acetone for 10 min at −20°C. After washing once in 80% methanol for 5 min at 4°C, sections were washed thrice with PBS at room temperature and blocked with 12% bovine serum albumin (in PBS) for 30 min. The primary antibody CD31 (BD Biosciences PharMingen) was added and incubated at room temperature for 3 h. After three additional washes with PBS, the sections were incubated in the dark for 30 min with the secondary antibody containing Alexa red (Molecular Probes/Invitrogen) and Hoechst dye 33342. Finally, sections were washed with PBS (3 × 5 min) and 10 min with 10 mmol/L Tris-HCl before embedding in Mowiol 4-88. Images were taken with the Zeiss microscope Axioskop 2 Plus (magnification, ×200) by an investigator (R.L.) not aware of the tumor/treatment group. Pictures were analyzed using the Image-Pro Plus software (Media Cybernetics). Four fields of each of five tumor samples in each group were analyzed.

Statistical analysis. All data are shown as mean plus SD if not indicated otherwise. The mean values of two groups were compared by *t* test. In the few cases where the variances differed significantly, the nonparametric Mann-Whitney *U* test was used and stated together with the *P* value. When more than two groups were compared, one-way ANOVA was used. A *P* value of <0.05 was considered significant.

Results

Recently, we identified genes whose expression in primary tumors is closely associated with the development of distant metastasis after tumor resection in human early-stage NSCLCs (8, 9). Because these genes might be suitable targets for novel adjuvant therapy approaches in NSCLC, we analyzed the

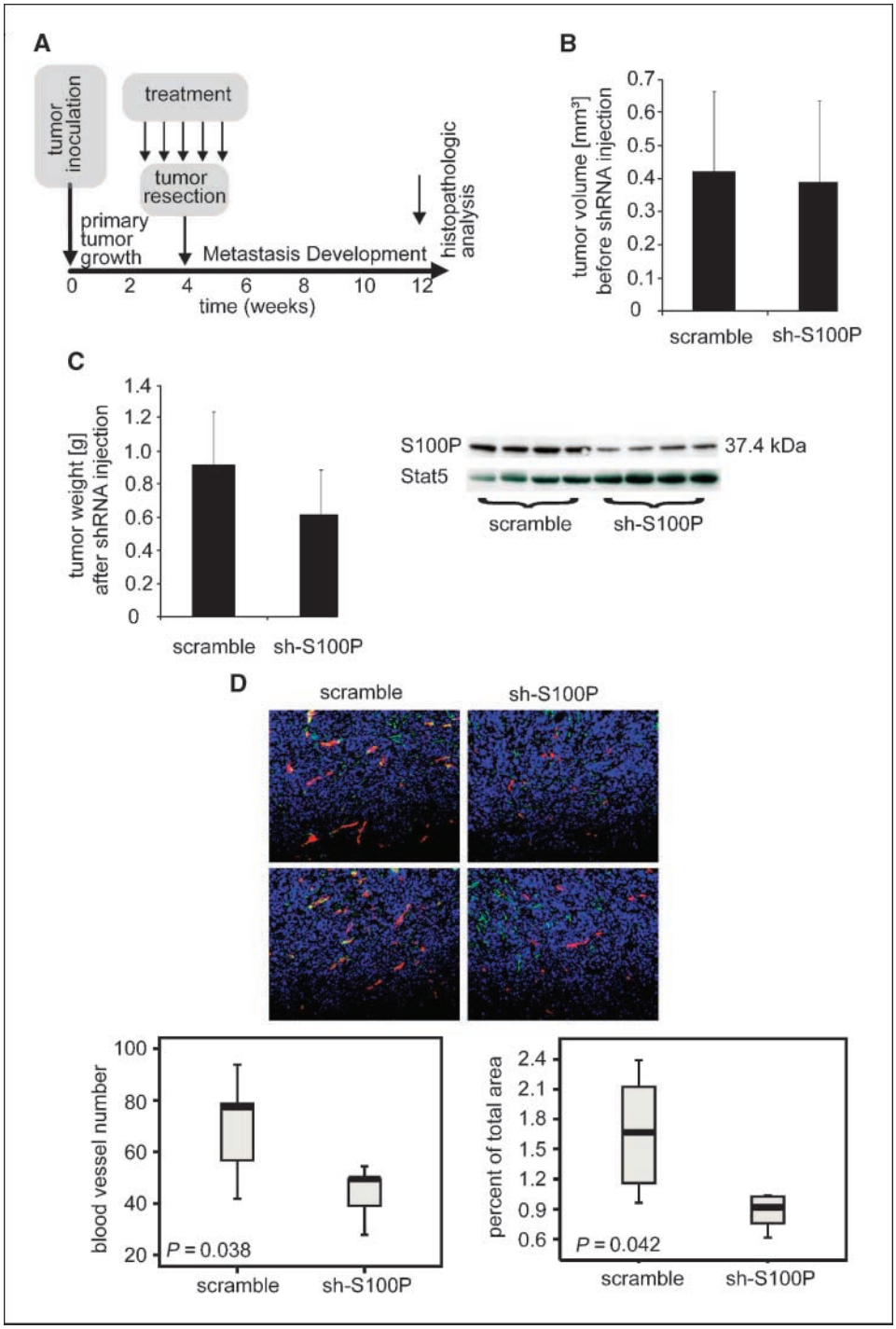

Figure 4. Effect of shRNA against S100P on tumor growth and angiogenesis. *A,* therapy approach in the mouse metastasis model. For neoadjuvant and adjuvant therapy, mice were treated with shRNA by injection into the tail vein twice in the week before surgery, during surgery, and twice in the week after tumor resection. Afterwards, the mice were monitored and sacrificed 12 wk after tumor inoculation (8 wk after tumor resection). *B,* the tumor volume was measured 3 wk after inoculation of S100P-expressing tumor cells. Mice were randomized to receive either shRNA-S100P or control shRNA therapy. *Columns,* mean values (n = 20, each); *bars,* SD. *C,* shRNA decreases S100P protein expression. *Left,* the tumor weight is shown after surgical excision following two i.v. injections with the indicated shRNA. *Columns,* mean values (n = 20, each); *bars,* SD (not significant). *Right,* Western blot analysis was performed on tumor lysates from mice treated with shRNA for S100P or control shRNA. A decreased protein expression of S100P is visible in all different tumor specimens from mice treated with shRNA-S100P. Stat5 served as a loading control. Densitometry (data not shown) showed a significant decrease (P = 0.029, Mann-Whitney test). *D,* angiogenesis is decreased in tumors from mice treated with shRNA against S100P. Frozen sections from tumors were double stained for CD31 (Alexa red) and SMA-1 (Alexa green). *Blue,* nuclei were visualized using DAPI counterstaining. *Top,* two representative examples of each treatment group are shown (magnification, ×200) and depict a decrease of blood vessels on shRNA-S100P treatment. *Bottom left,* the shRNA-S100P treatment reduced the number of blood vessels in primary tumors (P < 0.05). Computer-assisted analysis on red stainings provided the numerical result of total blood vessel numbers. Mean values were calculated from five independent tumors in each group with the help of the Image-Pro Plus software. *Bottom right,* down-regulation of S100P results in decreased blood vessel density (P < 0.05).

biological effects of these genes. For this purpose, the coding sequences were cloned in frame with EGFP to ease detection and to be able to compare expression levels. EIF4A1, SEC61β, as well as S100P were then expressed in HTB56 lung adenocarcinoma cells that are only weakly metastatic. Bulk cultures were used in all experiments to avoid clone-specific effects. Expression was confirmed by Western blot analysis, fluorescence microscopy, and flow cytometry (Fig. 1*A* and *B*; data not shown). None of the cell lines showed altered growth properties or proliferative advantages *in vitro* (data not shown). However, compared with the nontransfected cells or cells expressing EGFP alone, all of the studied genes significantly enhanced Transwell migration toward a high serum gradient (P = 0.026, ANOVA; Fig. 1*C*). Further assays were performed to analyze migration through an endothelial cell layer modeling transendothelial migration *in vivo* during metastasis. Two of three of the studied genes (*S100P* and *EIF4A1*) also led to enhanced transendothelial migration (Fig. 1*D*).

S100P and EIF4A1 were chosen to analyze their influence on metastasis formation *in vivo*.

Both genes were identified in primary tumors that metastasized following surgery in early-stage NSCLC. Therefore, we established a metastasis model that involved surgical removal after tumor formation resembling early-stage NSCLC treatment (Fig. 2*A*).

The NOD/SCID mice that were analyzed for the presence of distant metastasis in lungs (Fig. 2*B*) 8 weeks after surgery showed high frequency of metastasis in S100P-expressing tumors (8 of 12, 67%). In contrast, lungs from mice with control gene (EGFP)-transfected HTB56 cells harbored metastasis only in 2 of 12

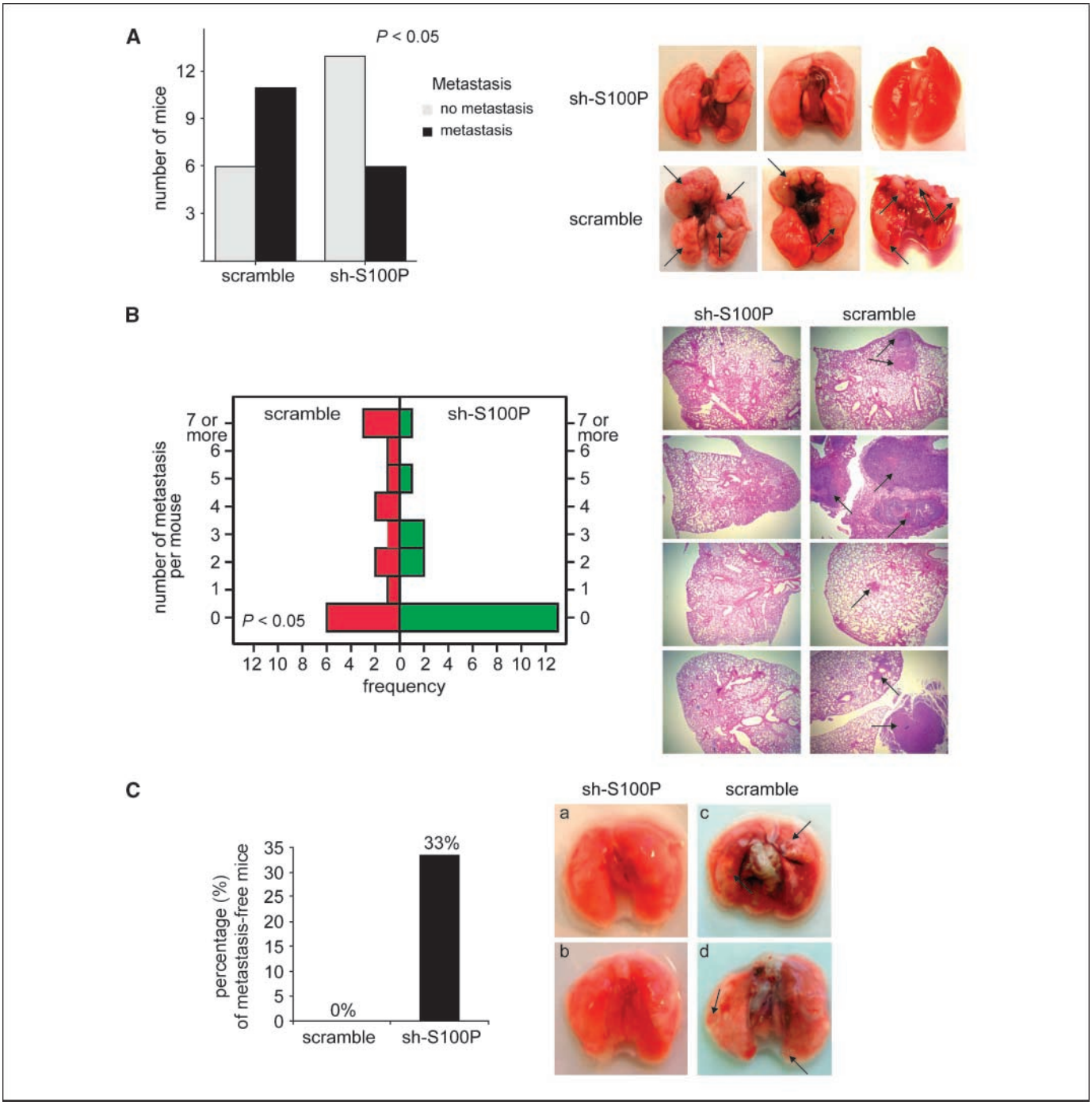

Figure 5. shRNA against S100P prevents metastasis formation in NOD/SCID mice. *A,* metastasis formation in lungs of NOD/SCID mice treated with shRNA for S100P and the scrambled control. *Left,* 65% of the mice (11 of 17) treated with scrambled shRNA and 32% of the mice (6 of 19) treated with shRNA against S100P developed lung metastasis ($P < 0.05$, Fischer's exact test); *right,* images of lungs from NOD/SCID mice treated with either shRNA-S100P or control shRNA. *Arrows,* metastasis. *B, left,* number of metastasis per mouse from lungs treated with shRNA-S100P or scramble ($P < 0.05$); *right,* hematoxylin-stained paraffin slides of lungs from NOD/SCID mice treated with shRNA-S100P or scrambled shRNA. *Arrows,* metastasis. *C,* shRNA-S100P prevents metastasis formation after i.v. injection of EGFP-HTB56 NSCLC cells. *Left,* NOD/SCID mice were i.v. injected with HTB56 cells expressing only EGFP and endogenous S100P and treated five times with 20 μg shRNA for S100P ($n = 9$) and the scrambled control ($n = 10$). shRNA-S100P prevented metastasis formation in three of nine mice (33%). *Right,* lungs of animals in a representative experiment. Lungs from mice treated with shRNA against S100P or scrambled are shown.

individuals (17%; $P < 0.009$). The metastasis rate was not enhanced in EIF4A1 cells (1 of 9, 11%). These findings established that only S100P enhances the metastatic phenotype of HTB56 NSCLC cells *in vivo*. Subsequent studies therefore focused on S100P.

Tumors, which were surgically removed 4 weeks after inoculation, still expressed the transgene as indicated by Western blot analyses and EGFP fluorescence of frozen sections (Fig. 2*C*). Importantly, S100P-expressing tumors showed significantly enhanced neoangiogenesis indicated by an increased number of vessels as well as an increase in the vessel area per visual field (Fig. 2*D*).

Because expression of S100P in early-stage NSCLC is associated with a poor prognosis and our functional analyses suggested a direct involvement in a metastatic phenotype, we evaluated the potential of shRNA-based adjuvant therapy. I.v. applied hairpin-based RNAi approaches have previously been shown to inhibit primary tumor growth *in vivo* (18). Therefore, we evaluated shRNA-based therapy against S100P. Published shRNAs against S100P (13) or the scrambled version (control) were tested *in vitro* and found to suppress mRNA levels in HTB58 cells and protein levels in BXPC-3 cells (Fig. 3*A*). On the protein level, endogenous S100P was not detectable in NSCLC cell lines. Therefore, we used BXPC-3 cells transfected with shRNA against S100P. The shRNAs were confirmed to be active *in vitro* and to inhibit migration of HTB58 cells through a transendothelial cell layer ($P = 0.029$; Fig. 3*B*). To analyze the specificity of the shRNAs targeting S100P, we analyzed expression of several S100 family members in the HTB58 and BXPC-3 cell lines transfected with either scrambled, shRNA-S100P1, or shRNA-S100P2 construct. No consistent repression in the mRNA levels was found for S100A2, S100A4, or S100A10 (Fig. 3*C*). On the other hand, lower levels of S100A8, S100A9, and S100A12 were present in cell lines transfected with either shRNA directed against S100P. The effects on S100A8, S100A9, and S100A12 proteins are likely to occur after the initial down-regulation of S100P because the shRNAs did not match to any sequence of either S100 gene. In addition, if off-target effects were relevant, it would be highly unlikely that both shRNAs against S100P would affect the same targets but would leave the other also related S100 proteins unaffected. These findings suggest that the S100P-shRNAs specifically target S100P.

(Neo-)adjuvant shRNA therapy using a mixture of both active shRNAs or scrambled control was administered i.v. using the metastasis model described above (Fig. 4*A*). First, we analyzed the effect of neoadjuvant shRNA therapy on the primary tumor (Fig. 4). HTB56 cells expressing S100P were s.c. injected into the right flanks of NOD/SCID mice. After 3 weeks of tumor growth, the mice were divided in two groups with similar tumor volumes (Fig. 4*B*). Mice were injected i.v. with 20 μg of shRNA plasmid against S100P (mixture of both shRNAs) or scrambled control sequence twice on the 4 days preceding the surgical removal of the tumor. After two shRNA treatments, a trend toward smaller tumor sizes at the time of surgery was noted (statistically not significant; Fig. 4*C*). Xenograft tumors from mice treated with S100P-shRNA showed reduced S100P protein levels compared with control shRNA–treated mice (Fig. 4*C*). In addition, angiogenesis was significantly inhibited (Fig. 4*D*). Blood vessel numbers ($P = 0.038$) and the blood vessel area ($P = 0.042$) significantly decreased after two shRNA-S100P injections. Angiogenesis was not altered by control shRNA compared with nontreated mice (compare Figs. 2*D* and 4*D*). No increase in IFN levels was found in plasma samples (data not shown).

In addition to analysis of the primary tumor, we also evaluated shRNA therapy in an adjuvant setting for its effect on metastasis (Fig. 5). At the time of surgery, a third i.v. injection was performed and two more adjuvant treatments were performed in the week following the surgery. Mice were followed up for a total of 8 weeks after surgery and metastasis development was evaluated by histologic examination in the mice (Fig. 4*A*). Although all organs were inspected, metastasis formation was restricted to the lungs with very few exceptions. Therefore, further analysis focussed on lung metastasis.

Metastasis developed in 11 of 17 (65%) of the mice treated with scrambled shRNA (Fig. 5*A*), consistent with the initial results of metastasis development in S100P-expressing tumor cells. In contrast, only 6 of 19 (32%) mice treated with S100P-shRNA developed metastasis ($P < 0.05$). Adjuvant therapy with shRNA against S100P reduced metastasis development by >50%. In addition, the average number of metastasis in individual mice was significantly decreased by S100P-shRNA ($P < 0.05$; Fig. 5*B*). Although these results were intriguing, two caveats remained: first, the metastasizing cells expressed ectopic S100P at relatively high levels, and second, shRNA against S100P also reduced albeit nonsignificantly the tumor size already at the time of surgery. The low metastatic capacity of cell lines without ectopic S100P expression precluded metastasis prevention assays of these cells in the s.c. model. Therefore, we also analyzed a more aggressive metastasis model of i.v. injection. For this, we used HTB56 cells only transfected with EGFP, which expressed low levels of endogenous S100P only. Lung metastasis development was analyzed 6 weeks after i.v. injection. In this system, 100% of the scrambled shRNA (control)-treated mice consistently developed metastasis (10 of 10). In contrast, 33% (3 of 9) of S100P-shRNA–treated mice did not develop metastasis (Fig. 5*C*).

Discussion

Adjuvant therapy can prevent metastasis formation. However, adjuvant therapy often fails to prevent metastasis development. The incomplete understanding of the metastatic process is the reason for the lack of specificity of the used therapeutic agents and the nonsatisfactory results in many cases. It is obvious that antiproliferative agents (e.g., classic cytotoxics) do not specifically target metastasis development. Hence, specific targeting of metastasis-inducing genes is a promising approach to improve cure rates in solid tumors.

For NSCLC, we and others have used microarray expression analysis as well as other genome-wide techniques to identify metastasis-related genes (8, 19–21). Many of the genes discovered in this process are likely to reflect the metastatic phenotype rather than actively contributing to it. Nonetheless, the discovery of genes associated with metastasis bears potential to discover novel prognostic markers and to identify novel therapeutic targets. The frequency of S100 proteins found as metastasis-associated genes is intriguing (8, 10, 13, 22, 23). Recently, we showed that S100P expression was closely associated with a significantly increased risk for NSCLC patients to develop distant metastasis (8). Here, we show that S100P confers a metastatic phenotype to NSCLC cell lines. The functions of the Ca^{2+}-binding S100 proteins are still incompletely understood. S100P might act intracellularly by binding to ezrin and provoking cytoskeleton alterations (24). It has also been shown that S100P is a secreted protein that might function by binding to the receptor of advanced glycation end

products (RAGE; ref. 25). Evidence for the latter point is also provided by recent findings that cromolyn blocks the S100P interaction with RAGE and inhibits pancreatic cancer growth and invasion (26).

We developed a xenograft mouse metastasis model to analyze the metastatic process in NSCLC and the potential to use the identified genes as therapeutic targets. Similar to patients with NSCLC, xenograft tumors were surgically removed and mice were followed for 8 additional weeks. In NSCLC cells without S100 protein expression, the metastasis rate was ~30%, which is comparable with the metastasis rate in stage I NSCLC patients. S100P expression doubled the metastasis rate and also enhanced angiogenesis in the xenograft tumors pointing toward the biological mechanisms of S100P action. The findings of increased angiogenesis are in line with extracellular S100P activities. Angiogenesis and the related lymphangiogenesis indicate a metastatic phenotype (27). In addition, recent reports suggest that other S100 proteins might stimulate metastasis development by enabling the formation of a premetastatic niche (28). Taken together, gene expression profiling studies and the functional analyses presented here and elsewhere provide convincing evidence that S100 proteins and especially S100P play a crucial role in metastasis development and could provide valuable drug targets.

Neoadjuvant and adjuvant cancer therapy is a promising area of investigation to increase survival in early-stage NSCLC. However, current therapy approaches show low efficacy and considerable side effects (29). Gene therapeutic approaches have been developed in NSCLC but these have not entered clinical practice (30). Thus far, few therapies have been developed that specifically target metastasis development in an adjuvant setting. Because S100P is closely involved in metastasis development, we performed proof-of-principle studies to determine whether hairpin RNAi is suitable for adjuvant therapy and whether blockade of S100P expression would prevent metastasis formation. Our findings provide evidence that i.v. application of shRNAs can prevent metastasis formation in a xenograft NSCLC model that resembles early-stage NSCLC with regard to tumor resection and (neo-)adjuvant therapy. In a 12-week study period, shRNA was administered i.v. twice before and after surgery as well as once during surgical resection. This adjuvant therapy approach is very similar to approaches feasible in actual patients. Importantly, shRNA specifically directed against S100P reduced the metastasis rate by ~50% compared with the same vector expressing a nonspecific control shRNA. Several approaches have shown *in vivo* activity of small interfering RNA delivered either as duplexes or as shRNA driven from plasmids. Naked plasmids have been used successfully, indicating that this is a feasible approach at least for some targets (18). The S100P-shRNA effects were tumor specific because no S100P homologue exists in mice. We also found a slightly decreased tumor weight after two neoadjuvant injections of shRNA directed against S100P at the time of surgery.

To exclude that the shRNA effectivity depended on this non-significant decrease of the resected tumor size, we administered the shRNA i.v. after i.v. injection of NSCLC lines with endogenous S100P expression. In these experiments, we observed that 33% of the mice could be prevented from metastasis development by shRNA-S100P, whereas 100% of the control shRNA–treated mice eventually developed metastasis. This observation hints toward effects of S100P-shRNA independent of the primary tumor size and against late steps in the metastatic process after invasion of the blood vessels by metastatic tumor cells.

Although these data indicate that shRNAs against S100P can be used as adjuvant therapies to specifically target metastasis, several problems remain. Several S100 proteins, such as S100P, S100A2, and S100A4, are likely to contribute to the metastatic phenotype. S100 proteins typically show 30% to 50% identity, but we did not find a unifying motif in metastasis-associated S100 proteins that separate them from nonmetastasis-associated S100 proteins. It might therefore be important to analyze the combination of shRNAs directed against different S100 proteins. The shRNAs used in this study were shown to specifically decrease mRNA and protein levels of their targets. Nonetheless, off-target effects cannot be ruled out entirely. Saturation of endogenous silencing pathways has recently been identified as an important source of shRNA-induced toxicity *in vivo* (31). In our study, mice were followed for up to 7 weeks after the last injection and we did not observe any detrimental effects. This is most likely due to the much less efficient delivery of naked plasmid compared with virus-induced cellular entry.

Taken together, these findings indicate for the first time that metastasis-inducing genes can be successfully targeted by shRNA *in vivo* and inhibit metastasis development. S100 proteins could provide attractive targets for specific inhibitory RNAs to develop an effective adjuvant therapy in solid tumors.

Acknowledgments

Received 6/26/2007; revised 11/8/2007; accepted 12/14/2007.

Grant support: NSCLC research in our laboratory is funded by the Deutsche Forschungsgemeinschaft MU1328/4-2. This project was partially supported by the Wilhelm Sander-Stiftung. C. Müller-Tidow is supported by a Heisenberg fellowship from the Deutsche Forschungsgemeinschaft. R. Liersch is supported by the Deutsche Forschungsgemeinschaft.

The costs of publication of this article were defrayed in part by the payment of page charges. This article must therefore be hereby marked *advertisement* in accordance with 18 U.S.C. Section 1734 solely to indicate this fact.

We thank Maria Schiller and Nicole Fehrmann for expert technical assistance, Drs. Arumugan and Logsdon for providing the shRNA-S100P sequence, and Drs. Johannes Roth and Dorothee Viemann for providing primer and probes for analyzing mRNA expression of several S100 proteins.

References

1. Steeg PS. Tumor metastasis: mechanistic insights and clinical challenges. Nat Med 2006;12:895–904.
2. SekidoY, Fong KM, Minna JD. Molecular genetics of lung cancer. Annu Rev Med 2003;54:73–87.
3. Mountain CF. Revisions in the international system for staging lung cancer. Chest 1997;111:1710–7.
4. MacRedmond R, McVey G, Lee M, et al. Screening for lung cancer using low dose CT scanning: results of 2 year follow up. Thorax 2006;61:54–6.
5. Winton T, Livingston R, Johnson D, et al. Vinorelbine plus cisplatin vs. observation in resected non-small-cell lung cancer. N Engl J Med 2005;352:2589–97.
6. Arriagada R, Bergman B, Dunant A, Le Chevalier T, Pignon JP, Vansteenkiste J. Cisplatin-based adjuvant chemotherapy in patients with completely resected non-small-cell lung cancer. N Engl J Med 2004;350:351–60.
7. Slamon DJ, Romond EH, Perez EA. Advances in adjuvant therapy for breast cancer. Clin Adv Hematol Oncol 2006;4 Suppl 1:4–9.
8. Diederichs S, Bulk E, Steffen B, et al. S100 family members and trypsinogens are predictors of distant metastasis and survival in early-stage non-small cell lung cancer. Cancer Res 2004;64:5564–9.
9. Ji P, Diederichs S, Wang W, et al. MALAT-1, a novel noncoding RNA, and thymosin β4 predict metastasis and survival in early-stage non-small cell lung cancer. Oncogene 2003;22:6087–97.
10. Wang G, Platt-Higgins A, Carroll J, et al. Induction of metastasis by S100P in a rat mammary model and its association with poor survival of breast cancer patients. Cancer Res 2006;66:1199–207.

11. Ohuchida K, Mizumoto K, Egami T, et al. S100P is an early developmental marker of pancreatic carcinogenesis. Clin Cancer Res 2006;12:5411–6.
12. Gibadulinova A, Barathova M, Kopacek J, et al. Expression of S100P protein correlates with and contributes to the tumorigenic capacity of HeLa cervical carcinoma cells. Oncol Rep 2005;14:575–82.
13. Arumugam T, Simeone DM, Van Golen K, Logsdon CD. S100P promotes pancreatic cancer growth, survival, and invasion. Clin Cancer Res 2005;11:5356–64.
14. Hamann MJ, Lubking CM, Luchini DN, Billadeau DD. Asef2 functions as a Cdc42 exchange factor and is stimulated by the release of an autoinhibitory module from a concealed C-terminal activation element. Mol Cell Biol 2007;27:1380–93.
15. Schwäble J, Choudhary C, Thiede C, et al. RGS2 is an important target gene of Flt3-ITD mutations in AML and functions in myeloid differentiation and leukemic transformation. Blood 2005;105:2107–14.
16. Müller-Tidow C, Diederichs S, Bulk E, et al. Identification of metastasis-associated receptor tyrosine kinases in non-small cell lung cancer. Cancer Res 2005;65:1778–82.
17. Kielbassa-Schnepp K, Strey A, Janning A, Missiaen L, Nilius B, Gerke V. Endothelial intracellular Ca^{2+} release following monocyte adhesion is required for the trans-endothelial migration of monocytes. Cell Calcium 2001; 30:29–40.
18. Spankuch B, Matthess Y, Knecht R, Zimmer B, Kaufmann M, Strebhardt K. Cancer inhibition in nude mice after systemic application of U6 promoter-driven short hairpin RNAs against PLK1. J Natl Cancer Inst 2004;96:862–72.
19. Raponi M, Zhang Y, Yu J, et al. Gene expression signatures for predicting prognosis of squamous cell and adenocarcinomas of the lung. Cancer Res 2006; 66:7466–72.
20. Potti A, Mukherjee S, Petersen R, et al. A genomic strategy to refine prognosis in early-stage non-small-cell lung cancer. N Engl J Med 2006;355:570–80.
21. Lu Y, Lemon W, Liu PY, et al. A gene expression signature predicts survival of patients with stage I non-small cell lung cancer. PLoS Med 2006;3:e467.
22. Kyriazanos ID, Tachibana M, Dhar DK, et al. Expression and prognostic significance of S100A2 protein in squamous cell carcinoma of the esophagus. Oncol Rep 2002;9:503–10.
23. Ford HL, Salim MM, Chakravarty R, Aluiddin V, Zain SB. Expression of Mts1, a metastasis-associated gene, increases motility but not invasion of a nonmetastatic mouse mammary adenocarcinoma cell line. Oncogene 1995;11:2067–75.
24. Koltzscher M, Neumann C, Konig S, Gerke V. Ca^{2+}-dependent binding and activation of dormant ezrin by dimeric S100P. Mol Biol Cell 2003;14:2372–84.
25. Arumugam T, Simeone DM, Schmidt AM, Logsdon CD. S100P stimulates cell proliferation and survival via receptor for activated glycation end products (RAGE). J Biol Chem 2004;279:5059–65.
26. Arumugam T, Ramachandran V, Logsdon CD. Effect of cromolyn on S100P interactions with RAGE and pancreatic cancer growth and invasion in mouse models. J Natl Cancer Inst 2006;98:1806–18.
27. Wissmann C, Detmar M. Pathways targeting tumor lymphangiogenesis. Clin Cancer Res 2006;12:6865–8.
28. Hiratsuka S, Watanabe A, Aburatani H, Maru Y. Tumour-mediated upregulation of chemoattractants and recruitment of myeloid cells predetermines lung metastasis. Nat Cell Biol 2006;8:1369–75.
29. Kassam F, Shepherd FA, Johnston M, et al. Referral patterns for adjuvant chemotherapy in patients with completely resected non-small cell lung cancer. J Thorac Oncol 2007;2:39–43.
30. Schuler M, Herrmann R, De Greve JL, et al. Adenovirus-mediated wild-type p53 gene transfer in patients receiving chemotherapy for advanced non-small-cell lung cancer: results of a multicenter phase II study. J Clin Oncol 2001;19:1750–8.
31. Grimm D, Streetz KL, Jopling CL, et al. Fatality in mice due to oversaturation of cellular microRNA/short hairpin RNA pathways. Nature 2006;441: 537–41.